Available online at www.sciencedirect.com

ScienceDirect

Ceramics International 38 (2012) 1765–1769

CERAMICS INTERNATIONAL

www.elsevier.com/locate/ceramint

Preparation and properties of $CdSiO_3$: Mn^{2+}, Tb^{3+} phosphor

Xiaofei Qu, Lixin Cao *, Wei Liu, Ge Su

Institute of Materials Science and Engineering, Ocean University of China, Songling Road 238, Qingdao 266100, Shandong Province, PR China

Received 3 April 2011; received in revised form 29 May 2011; accepted 31 May 2011
Available online 12 June 2011

Abstract

$CdSiO_3$: Mn^{2+}, Tb^{3+} long-lasting phosphor was prepared by the conventional high temperature solid-state method. Effects of the content of Mn^{2+} and Tb^{3+} on the luminescent properties of phosphor $CdSiO_3$: Mn^{2+}, Tb^{3+} were investigated by means of photoluminescence (PL) spectra, the afterglow intensity decay curves and the thermoluminescence (TL) spectra. It was found that when the Mn^{2+} and Tb^{3+} dopant-concentrations were 0.4 mol% and 0.8 mol% of Cd^{2+} ions in $CdSiO_3$, respectively, the luminescence of phosphor prepared had better luminescent property and longer afterglow time. Role of Tb^{3+} co-doped into $CdSiO_3$: Mn^{2+} matrix was discussed in this paper.

Keywords: Silicate phosphor; Afterglow; Photoluminescence

1. Introduction

Long lasting phosphor is a kind of energy-storing material, which can absorb the visible or ultraviolet lights, store the energy, and then release the energy as visible light that leads to a long lasting afterglow in the darkness. The material can be used in many fields, including traffic signs, interior decoration, and light sources [1–4]. The practical phosphors were focused mainly on some oxygen-containing inorganic compounds [5], such as oxides, aluminates, borates, aluminoborate and silicates. They usually have suitable host absorption band, which can be used by luminescent center. Compared to the other phosphors, silicate ones have been paid considerable attention because of their high chemical stability, water-resistant property and new properties of afterglow [6–11].

Theoretically, the long-afterglow emitting of phosphors arises from the emission of the impurity centers. If there are adequate hole and/or electron traps with suitable depth values within the host lattice, long-afterglow emission can be observed in the impurity-doped phosphors. To date, it is well-known that the luminescent properties of phosphors are strongly dependent on the kind of dopant ion and the crystal structure of the host lattice [12].

As we all know, the crystal structure of $CdSiO_3$ is expected to be one-dimensional chain of edge-sharing SiO_4 tetrahedron. It is very easy to implant other ions into the host lattice and create traps located at suitable depths that can store the excitation energy and emit light at room temperature [13].

Rare-earth-activated phosphors have attracted much attention for their well-defined transitions within the 4f shell [14–18]. Beside the rare-earth ions-doped phosphors, the manganese ions-doped materials are good candidates for photonic sources. Many researchers have studied the luminescence behaviors of the Mn^{2+} activator [19–23].

In this work, new long-lasting phosphor $CdSiO_3$: Mn^{2+}, Tb^{3+} was synthesized at 1050 °C via solid-state reaction method. The luminescence properties, including photoluminescence (PL) spectra, the afterglow intensity decay curves and the thermoluminescence (TL) spectra, were studied.

2. Experimental procedure

The $CdSiO_3$: Mn^{2+}, Tb^{3+} phosphor was prepared by the conventional high temperature solid-state method. The starting materials were $CdCO_3$ (A.R.), SiO_2 (G.R.), $MnCO_3$ (A.R.) and Tb_4O_7 (>99.99%). Both Mn^{2+} and Tb^{3+} dopant-concentrations relative to the host compound were chosen to be varied from 0 mol% to 1.0 mol%, respectively. The starting materials were mixed well, grinded, and then calcined at 1050 °C for 3 h. The excitation and emission spectra were

* Corresponding author. Tel.: +86 532 66781901; fax: +86 532 66781320.
E-mail address: caolixin@mail.ouc.edu.cn (L. Cao).

0272-8842/$36.00 © 2011 Published by Elsevier Ltd and Techna Group S.r.l.
doi:10.1016/j.ceramint.2011.05.143

measured by a Flurolog-3-21 fluorescence spectrophotometer equipped with 150 W Xenon lamp as excitation source. The afterglow intensity decay curve was measured on the same instrument. The excitation light was blocked when the samples had been exposed for 1 min under 254 nm UV light and the emitted afterglow from them were recorded over a time period of 1–120 s in the kinetic analysis mode of the spectrometer system. The scan interval was set to 0.5 s. The thermoluminescence (TL) spectra were recorded as the temperature rose linearly with a heating rate of 5 °C/s within the range 35–320 °C with a thermal luminescence detector reader (made by Beijing Nuclear Instrument Factory, China). The thermoluminescence (TL) spectra of the samples were measured after irradiation with a standard UV lamp peak at 254 nm with a power of 15 W at room temperature. All measurements were carried out at room temperature (RT) except for the TL spectra.

3. Results and discussion

Fig. 1 shows the photoluminescence spectra of $CdSiO_3$ co-doped with Mn^{2+} and Tb^{3+}, where the concentration of Mn^{2+} was fixed at 1.0% and that of Tb^{3+} varied from 0.1% to 1.0%. The excitation spectra were obtained by scanning wavelengths from 200 to 400 nm monitored at 587 nm. The emission spectra were scanned from 400 to 700 nm while excited at 286 nm. In the emission spectra, a broad band centered at about 587 nm which could be seen in all these phosphors, could be attributed to the ${}^4T_{1g}(G) \rightarrow {}^6A_{1g}(S)$ transition of Mn^{2+} ions occupying the Cd^{2+} sites in the lattice [24]. The emission intensity of Mn^{2+} decreased for samples with higher concentration of Tb^{3+}, attributing to the quenching effect of Tb^{3+} on Mn^{2+}. When the content of Tb^{3+} was 0.5%, the sample photoluminescence intensity was highest. In the excitation spectra, a broad band centered at about 286 nm which could be seen in the phosphors,

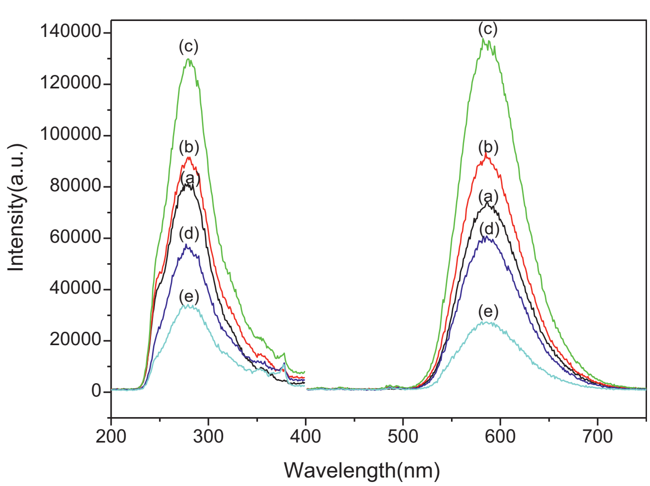

Fig. 1. Photoluminescence spectra of $CdSiO_3$: 1.0% Mn^{2+}, Tb^{3+} series with different concentration: (a) $CdSiO_3$: 1.0% Mn^{2+}, 0.1% Tb^{3+}; (b) $CdSiO_3$: 1.0% Mn^{2+}, 0.3% Tb^{3+}; (c) $CdSiO_3$: 1.0% Mn^{2+}, 0.5% Tb^{3+}; (d) $CdSiO_3$: 1.0% Mn^{2+}, 0.8% Tb^{3+}; and (e) $CdSiO_3$: 1.0% Mn^{2+}, 1.0% Tb^{3+} (λ_{ex} = 286 nm, λ_{em} = 587 nm).

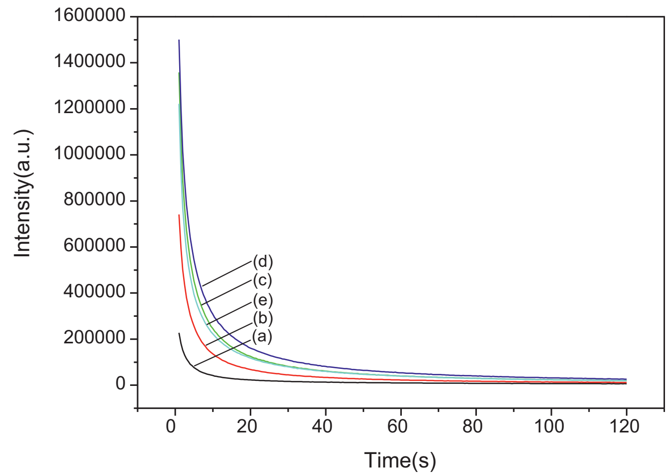

Fig. 2. The afterglow decay curves of $CdSiO_3$: 1.0% Mn^{2+}, Tb^{3+} series with different concentration of Tb^{3+}: (a) $CdSiO_3$: 1.0% Mn^{2+}, 0.1% Tb^{3+}; (b) $CdSiO_3$: 1.0% Mn^{2+}, 0.3% Tb^{3+}; (c) $CdSiO_3$: 1.0% Mn^{2+}, 0.5% Tb^{3+}; (d) $CdSiO_3$: 1.0% Mn^{2+}, 0.8% Tb^{3+}; and (e) $CdSiO_3$: 1.0% Mn^{2+}, 1.0% Tb^{3+} at 587 nm.

could be attributed to the host absorption. For $CdSiO_3$: Mn^{2+}, Tb^{3+}, two peaks (353 and 378 nm), resulting from transitions of Tb^{3+}, (${}^7F_6$–${}^5D_2$) and (${}^7F_6$–${}^5D_3$), could be seen [25–31]. The intensity of ~286 nm broad band in all co-doped samples was higher than that of the other peaks, which indicated that the host absorption played the leading role in the emission of Mn^{2+} ions. The energy was first absorbed by the host then transferred to the luminescence center.

Fig. 2 shows the afterglow intensity decay curves of Mn^{2+}, Tb^{3+} co-doped $CdSiO_3$ phosphors. The phosphorescence emission intensity of all samples decreased quickly at first and then slowly. At first, the afterglow intensity for (c) $CdSiO_3$: 1.0% Mn^{2+}, 0.5% Tb^{3+}, (d) $CdSiO_3$: 1.0% Mn^{2+}, 0.8% Tb^{3+}, and (e) $CdSiO_3$: 1.0% Mn^{2+}, 1.0% Tb^{3+} is higher than that of the two others. When the time is up to 40 s, compared to the other samples, $CdSiO_3$: 1.0% Mn^{2+}, 0.8% Tb^{3+} still showed higher afterglow intensity and the situation kept to the end of the measurement. So, the afterglow performance for the $CdSiO_3$: 1.0% Mn^{2+}, 0.8% Tb^{3+} phosphor was best and the phosphorescence for the $CdSiO_3$: 1.0% Mn^{2+}, 0.8% Tb^{3+} phosphor could be seen with the naked eye in the dark for more than 0.5 h after the removal of the 254 nm UV light.

The phosphorescence spectra of co-doped samples at the recorded decay time of 1 min after the removal of the excitation source are shown in the inset of Fig. 3. Although the emission of Tb^{3+} (486 nm) still exist in the phosphorescence spectra, the emission of Mn^{2+} (587 nm) was detected mainly in the co-doped sample in the decay process. Furthermore, for all samples, the shapes of the bands were similar, which indicated that Mn^{2+} ions were the activator and Tb^{3+} ions in the samples played the role of the assistant activator. From the figure, we could also see that the order of intensity of Mn^{2+} (587 nm) was (a) < (b) < (e) < (c) < (d). Thus, the co-doped samples represented orange afterglow and the sample $CdSiO_3$: 1.0% Mn^{2+}, 0.8% Tb^{3+} was the brightest, consisting with Fig. 2. The results also indicated that the afterglow performance could be better with proper electron traps resulting from proper Tb^{3+} dopant.

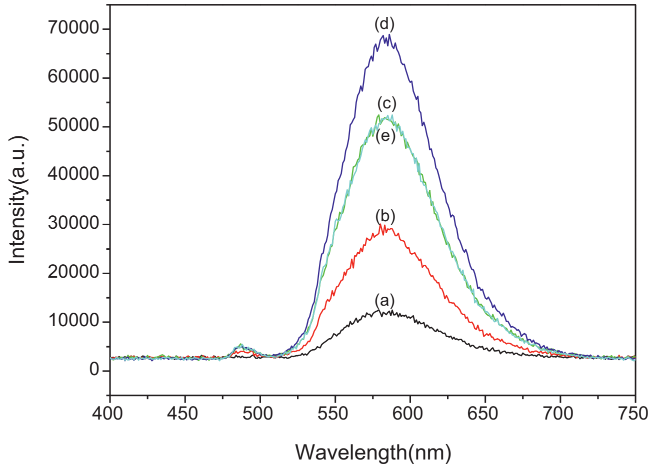

Fig. 3. Phosphoresence spectra of $CdSiO_3$: 1.0% Mn^{2+}, Tb^{3+} series with different concentration of Tb^{3+}: (a) $CdSiO_3$: 1.0% Mn^{2+}, 0.1% Tb^{3+}; (b) $CdSiO_3$: 1.0% Mn^{2+}, 0.3% Tb^{3+}; (c) $CdSiO_3$: 1.0% Mn^{2+}, 0.5% Tb^{3+}; (d) $CdSiO_3$: 1.0% Mn^{2+}, 0.8% Tb^{3+}; and (e) $CdSiO_3$: 1.0% Mn^{2+}, 1.0% Tb^{3+}.

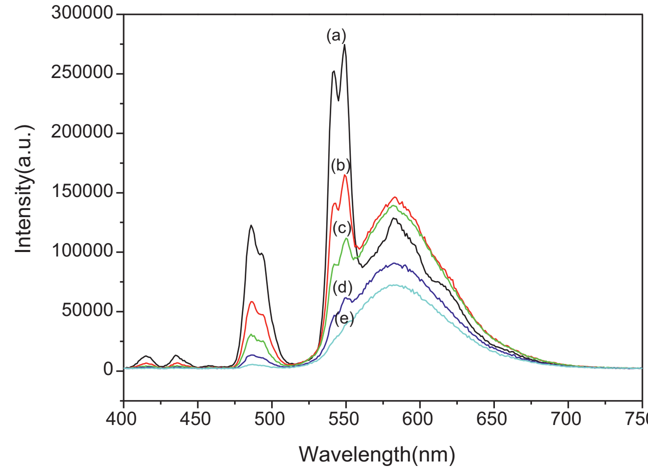

Fig. 5. Phosphoresence spectra of $CdSiO_3$: Mn^{2+}, 0.8% Tb^{3+} series with different concentration of Mn^{2+}: (a) $CdSiO_3$: 0.8% Tb^{3+}, 0.2% Mn^{2+}; (b) $CdSiO_3$: 0.8% Tb^{3+}, 0.4% Mn^{2+}; (c) $CdSiO_3$: 0.8% Tb^{3+}, 0.6% Mn^{2+}; (d) $CdSiO_3$: 0.8% Tb^{3+}, 0.8% Mn^{2+}; and (e) $CdSiO_3$: 0.8% Tb^{3+}, 1.0% Mn^{2+}.

In order to find out the optimal concentration of Mn^{2+} for the better luminescence property, the afterglow intensity decay curves of $CdSiO_3$: Mn^{2+}, Tb^{3+} with different Mn^{2+} concentration are shown in Fig. 4. The phosphorescence emission intensity of all samples decreased quickly at first and then slowly. The afterglow intensity for these samples increased at first (1 s) as follows: (e) < (d) < (a) < (b) < (c), while the order of intensity changed after the removal of the excitation light for 11 s, and since then, the order of intensity was always (e) < (d) < (a) < (c) < (b) to the end of the recorded time. Among all the samples, the afterglow performance for the $CdSiO_3$: 0.8% Tb^{3+}, 0.4% Mn^{2+} phosphor was best and the phosphorescence for it could be seen with the naked eye in the dark for more than 1 h after the removal of the 254 nm UV light.

The phosphorescence spectrum of $CdSiO_3$: Mn^{2+}, Tb^{3+} with different Mn^{2+} concentration at the recorded decay time of 1 min after the removal of the excitation source are shown in the inset of Fig. 5. In the phosphorescence spectrum, beside the emission of Mn^{2+} (587 nm), four peaks (415, 435, 486 and 548 nm) resulting from transitions of Tb^{3+}, ($^5D_3 \rightarrow {}^7F_5$), ($^5D_3 \rightarrow {}^7F_4$), ($^5D_4 \rightarrow {}^7F_6$) and ($^5D_4 \rightarrow {}^7F_5$), could also be seen [32–51]. With the Mn^{2+} concentration increasing (0.2–1.0%), the Mn^{2+} afterglow intensity for the co-doped $CdSiO_3$ samples was higher at first and then lower. The order of Mn^{2+} (587 nm) afterglow intensity was: (e) < (d) < (a) < (c) < (b), which consisted with Fig. 4.

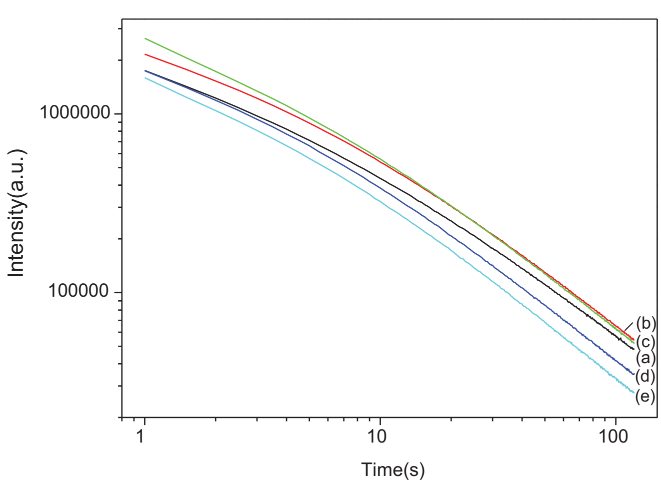

Fig. 4. The afterglow decay curves of $CdSiO_3$: Mn^{2+}, 0.8% Tb^{3+} series with different concentration of Mn^{2+}: (a) $CdSiO_3$: 0.8% Tb^{3+}, 0.2% Mn^{2+}; (b) $CdSiO_3$: 0.8% Tb^{3+}, 0.4% Mn^{2+}; (c) $CdSiO_3$: 0.8% Tb^{3+}, 0.6% Mn^{2+}; (d) $CdSiO_3$: 0.8% Tb^{3+}, 0.8% Mn^{2+}; and (e) $CdSiO_3$: 0.8% Tb^{3+}, 1.0% Mn^{2+}.

The afterglow intensity decay curves of the phosphorescence at 587 nm in the $CdSiO_3$: 1.0% Mn^{2+}, 0.5% Tb^{3+} and $CdSiO_3$: 1.0% Mn^{2+} are shown in the inset of Fig. 6. The afterglow performance for $CdSiO_3$: 1.0% Mn^{2+} was not good. A little afterglow could be seen for $CdSiO_3$: 1.0% Mn^{2+} samples, but $CdSiO_3$: Mn^{2+} samples co-doped with Tb^{3+} had higher phosphorescence intensity and longer decay time than only Mn^{2+} doped ones. Furthermore, we could see that co-doped Tb^{3+} ions increased the initial phosphorescence intensity of the sample.

In order to explain the enhancement afterglow process of Tb^{3+}-doped in $CdSiO_3$: Mn^{2+}, it is necessary to take the TL spectra into consideration. Fig. 6 shows the TL curves of $CdSiO_3$:

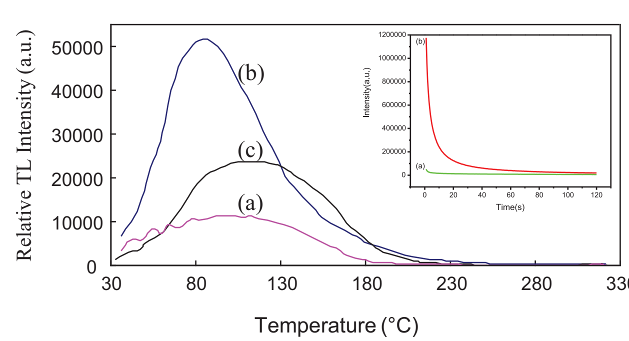

Fig. 6. TL spectra of (a) $CdSiO_3$: 1.0% Mn^{2+}; (b) $CdSiO_3$: 1.0% Mn^{2+}, 0.5% Tb^{3+}; (c) $CdSiO_3$: 0.5% Tb^{3+}. The inset displays the afterglow decay curves of (a) $CdSiO_3$: 1.0% Mn^{2+} and (b) $CdSiO_3$: 1.0% Mn^{2+}, 0.5% Tb^{3+} at 587 nm.

1.0% Mn^{2+}, $CdSiO_3$: 1.0% Mn^{2+}, 0.5% Tb^{3+} and $CdSiO_3$: 0.5% Tb^{3+} samples. The TL spectra of $CdSiO_3$: 1.0% Mn^{2+}, $CdSiO_3$: 1.0% Mn^{2+}, 0.5% Tb^{3+} and $CdSiO_3$: 0.5% Tb^{3+}consisted one primary peak at 97, 85 and 115 °C, respectively. It could be explained by the difference in ionic radii between Cd^{2+} and Tb^{3+}. The ionic radii of Cd^{2+}, Mn^{2+}, Tb^{3+}, Si^{4+} were 0.097, 0.081, 0.0923 nm and 0.041 nm, respectively. The Tb^{3+} ions are expected to occupy the Cd^{2+} sites in the $CdSiO_3$: Mn^{2+} host and no Tb^{3+} ion is expected to occupy the Si^{4+} sites. Since the Tb^{3+} ionic radius is smaller than the Cd^{2+} ionic radius, it is easy for it to substitute Cd^{2+} site. Due to the nonequivalent substitution, an excess of positive charge in the lattice must be compensated [52]. There are two possible ways to fulfill the charge compensation of the Tb^{3+} co-doped in $CdSiO_3$: Mn^{2+} phosphor. One possible way to fulfill the charge compensation of the Tb^{3+} co-doped in $CdSiO_3$: Mn^{2+} phosphor was that two Tb^{3+} ions replace three Cd^{2+} ions to balance the charge of the phosphor, which created two $Tb^{\bullet}_{Cd}$ positive defects and one V''_{Cd} negative defect ($2Tb^{3+} \rightarrow 3Cd^{2+}$). In addition, because of the relatively high vapor pressure of the Cd^{2+} component, the vacancies of Cd^{2+} (V''_{Cd}) could also derive from the synthesis process [53]. All these vacancies make up a trap level.

The TL intensity of $CdSiO_3$: 1.0% Mn^{2+}, $CdSiO_3$: 1.0% Mn^{2+}, 0.5% Tb^{3+} and $CdSiO_3$: 0.5% Tb^{3+} increased as follows: $CdSiO_3$: 1.0% Mn^{2+} < $CdSiO_3$: 0.5% Tb^{3+} < $CdSiO_3$: 1.0% Mn^{2+}, 0.5% Tb^{3+}, indicating that more traps were created when Tb^{3+} doped in $CdSiO_3$: Mn^{2+}. It implied that the ionic radii of the foreign co-doped ions play an important role of traps formation.

4. Conclusion

In conclusion, long-lasting phosphorescence was observed in $CdSiO_3$: Mn^{2+}, Tb^{3+} powder samples prepared by solid-state reaction. The luminescence of phosphors prepared under the condition of the content of Mn^{2+} 0.4 mol% and Tb^{3+} 0.8 mol% had better luminescent property and longer afterglow time. The phosphorescence for it could be seen with the naked eye for more than 1 h in the dark after the removal of the 254 nm UV light. Some Tb^{3+} ions in $CdSiO_3$: Mn^{2+}, Tb^{3+} acted as a role of the assistant activator.

Acknowledgements

We would like to thank the National Science Foundation of China (NSFC 50672089), the Program for New Century Excellent Talents in University (NCET-08-0511) and the Outstanding Adult-Young Scientific Research Encouraging Foundation of Shandong Province (BS2010CL049) for their financial support.

References

[1] L. Lin, C.S. Shi, Z.F. Wang, W.P. Zhang, M. Yin, A kinetics model of red long-lasting phosphorescence in $MgSiO_3$: Eu^{2+}, Dy^{3+}, Mn^{2+}, J. Alloys Compd. 466 (2008) 546–550.

[2] L. Lin, M. Yin, C.S. Shi, W.P. Zhang, Luminescence properties of a new red long-lasting phosphor: Mg_2SiO_4: Dy^{3+}, Mn^{2+}, J. Alloys Compd. 455 (2008) 327–330.

[3] T.P. Tang, C.M. Lee, F.C. Yen, The photoluminescence of $SrAl_2O_4$: Sm phosphors, Ceram. Int. 32 (2006) 665–671.

[4] S.L. Yuan, Y.X. Yang, B. Fang, G.R. Chen, Effects of doping ions on afterglow properties of Y_2O_2S: Eu phosphors, Opt. Mater. 30 (2007) 535–538.

[5] H. Liang, J. Shi, Q. Su, S. Zhang, Y. Tao, Spectroscopic properties of Ce^{3+} doped $MBPO_5$ (M = Ca, Sr, Ba) under VUV excitation, Mater. Chem. Phys. 92 (2005) 180–184.

[6] H.Y. Wu, Y.H. Hu, Y.H. Wang, C.J. Fu, The luminescent properties of the substitution of Ho^{3+} for Dy^{3+} in the $M_2MgSi_2O_7$: Eu^{2+}, Dy^{3+} (M: Sr, Ca) long afterglow phosphors, Mater. Sci. Eng., B 172 (2010) 276–282.

[7] V.B. Bhatkar, S.K. Omanwar, S.V. Moharil, Combustion synthesis of silicate phosphors, Opt. Mater. 29 (2007) 1066–1070.

[8] Y. Ito, A. Komeno, K. Uematsu, K. Toda, M. Sato, Luminescence properties of long-persistence silicate phosphors, J. Alloys Compd. 408–412 (2006) 907–910.

[9] H.S. Kang, Y.C. Kang, K.Y. Jung, S.B. Park, Eu-doped barium strontium silicate phosphor particles prepared from spray solution containing NH_4Cl flux by spray pyrolysis, Mater. Sci. Eng., B 121 (2005) 81–85.

[10] J.S. Kim, S.W. Mho, Y.H. Park, J.C. Choi, H.L. Park, G.S. Kim, White-light-emitting Eu^{2+} and Mn^{2+}-codoped silicate phosphors synthesized through combustion process, Solid State Commun. 136 (2005) 504–507.

[11] Y.L. Ding, Y.X. Zhang, Z.Y. Wang, W. Li, D.L. Mao, H.B. Han, C.K. Chang, Photoluminescence of Eu single doped and Eu/Dy codoped $Sr_2Al_2SiO_7$ phosphors with long persistence, J. Lumin. 129 (2009) 294–299.

[12] C.B. Liu, G.B. Che, Z.L. Xu, Q.W. Wang, Luminescence properties of a Tb^{3+} activated long-afterglow phosphor, J. Alloys Compd. 474 (2009) 250–253.

[13] L. Zhang, G.Y. Hong, X.L. Sun, The luminescence of the phosphor Sr_2ZrO_4 with one-dimensional chains structure, Chin. Chem. Lett. 10 (1999) 799–802.

[14] S. Sivakumar, F.C.J.M. VanVeggel, M. Raudsepp, Bright white light through up-conversion of a single NIR source from solgel-derived thin film made with Ln^{3+}-doped LaF_3 nanoparticles, J. Am. Chem. Soc. 127 (2005) 12464–12465.

[15] J.F. Suyver, J. Grimm, K.W. Krämer, H.U. Güdel, Highly efficient near-infrared to visible up-conversion process in $NaYF_4$: Er^{3+}, Yb^{3+}, J. Lumin. 114 (2005) 53–59.

[16] J.A. Capobianco, F. Vetrone, J.C. Boyer, A. Speghini, M. Bettinelli, Visible upconversion of Er^{3+} doped nanocrystalline and bulk Lu_2O_3, Opt. Mater. 19 (2002) 259–268.

[17] C. Feldmann, T. Jüstel, C.R. Ronda, P.J. Schmidt, Inorganic luminescent materials: 100 years of research and application, Adv. Funct. Mater. 13 (2003) 511–516.

[18] R.C. Evans, L.D. Carlos, P. Rocha, J. Douglas, Tuning the emission colour in mixed lanthanide microporous silicates: energy transfer, composition and chromaticity, J. Mater. Chem. 18 (2008) 1100–1107.

[19] R. Morimo, R. Mochinaga, K. Nakamura, Preparation and characterization of a manganese activated zinc silicate phosphor by fume pyrolysis of an alkoxide solution [Zn_2SiO_4: Mn], Mater. Res. Bull. 29 (1994) 751–757.

[20] C.R. Ronda, T. Amrein, Evidence for exchange-induced luminescence in Zn_2SiO_4: Mn, J. Lumin. 69 (1996) 245–248.

[21] K.N. Kim, H.K. Jung, H.D. Park, D.J. Kim, High luminance of new green emitting phosphor, Mg_2SnO_4: Mn, J. Lumin. 99 (2002) 169–173.

[22] J.X. Wan, Z.H. Wang, X.Y. Chen, L. Mu, W.C. Yu, Y.T. Qian, Controlled synthesis and relationship between luminescent properties and shape/crystal structure of Zn_2SiO_4: Mn^{2+} phosphor, J. Lumin. 121 (2006) 32–38.

[23] B.F. Lei, Y.L. Liu, Z.R. Ye, C.S. Shi, Luminescence properties of $CdSiO_3$: Mn^{2+} phosphor, J. Lumin. 109 (2004) 215–219.

[24] J. Ramirez-Serrano, E. Madrigal, F. Ramos, G.U. Caldino, Optical spectroscopy of Mn^{2+} ions in $CdCl_2$ single crystals, J. Lumin. 71 (1997) 169–175.

[25] Z.J. Zhang, J.L. Yuan, S. Chen, H.H. Chen, X.X. Yang, J.T. Zhao, G.B. Zhang, C.S. Shi, Investigation on the luminescence of RE^{3+} (RE = Ce, Tb, Eu and Tm) in $KMGd(PO_4)_2$ (M = Ca, Sr) phosphates, Opt. Mater. 30 (2008) 1848–1853.

[26] L.Y. Zhou, W.C.H. Choy, J.X. Shi, M.L. Gong, H.B. Liang, A novel green emitting phosphor $Ca_{1.5}Y_{1.5}Al_{3.5}Si_{1.5}O_{12}$: Tb^{3+}, Mater. Chem. Phys. 100 (2006) 372–374.

[27] A. Bao, C.Y. Tao, H. Yang, Luminescent properties of nanoparticles $LaSrAl_3O_7$: RE^{3+} (RE = Eu, Tb) via the citrate sol–gel method, J. Mater. Sci.: Mater. Electron. 19 (2008) 476–481.

[28] Z.Y. Ren, C.Y. Tao, H. Yang, Synthesis and luminescent characterization of $YAl_3(BO_3)_4$:Tb^{3+} phosphors, J. Mater. Sci.: Mater. Electron. 19 (2008) 319–321.

[29] T.W. Kuo, T.M. Chen, Synthesis and luminescence properties of Eu^{3+}, Ce^{3+} and Tb^{3+}-activated $Sr_3La_2(BO_3)_4$ under UV excitation, J. Lumin. 130 (2010) 483–487.

[30] H.J. Meyer, L. Kienle, A.M. Kłonkowski, Tb^{3+} luminescence enhancement of YAG: Tb^{3+} nanocrystals embedded in silica xerogel, J. Non-Cryst. Solids 355 (2009) 1333–1337.

[31] X.M. Liu, J. Lin, Synthesis and luminescent properties of $LaInO_3$: RE^{3+} (RE = Sm, Pr and Tb) nanocrystalline phosphors for field emission displays, Solid State Sci. 11 (2009) 2030–2036.

[32] Z.Y. Zhang, Y.H. Zhang, X.L. Li, J.H. Xu, Y. Huang, VUV–UV luminescence of magnetoplumbite: $(Sr_{0.96-x}Ba_{0.04})Al_{12-y}Mg_yO_{19}$:$Tb_x$, J. Lumin. 128 (2008) 476–480.

[33] H.C. Yang, C.Y. Li, Y. Tao, J.H. Xu, G.B. Zhang, Q. Su, The luminescence of $CaYBO_4$: RE^{3+} (RE = Eu, Gd, Tb, Ce) in VUV–visible region, J. Lumin. 126 (2007) 196–202.

[34] B. Yan, H.H. Huang, Matrix-inducing synthesis and luminescence of Zn_2SiO_4:$x$$Tb^{3+}$ submicrometer phosphors derived from the sol–gel assembling of different multicomponent hybrid precursors, J. Alloys Compd. 429 (2007) 338–342.

[35] C.J. Duan, H.H. Chen, X.X. Yang, J.T. Zhao, Luminescence properties of Eu^{3+}, Tb^{3+} or Tm^{3+} activated $Ca_4GdO(BO_3)_3$ under X-ray and UV excitation, Opt. Mater. 28 (2006) 956–961.

[36] Z.H. Li, J.H. Zeng, G.C. Zhang, Y.D. Li, A new promising phosphor, $Na_3La_2(BO_3)_3$:Ln (Ln = Eu, Tb), J. Solid State Chem. 178 (2005) 3624–3630.

[37] C.C. Yu, M. Yu, C.X. Li, X.M. Liu, J. Yang, P.P. Yang, J. Lin, Facile sonochemical synthesis and photoluminescent properties of lanthanide orthophosphate nanoparticles, J. Solid State Chem. 182 (2009) 339–347.

[38] Y.P. Naik, M. Mohapatra, N.D. Dahale, T.K. Seshagiri, V. Natarajan, S.V. Godbole, Synthesis and luminescence investigation of RE^{3+} (Eu^{3+}, Tb^{3+} and Ce^{3+})-doped lithium silicate (Li_2SiO_3), J. Lumin. 129 (2009) 1225–1229.

[39] S.S. Sanaye, B.S. Dhabekar, R. Kumar, S.N. Menon, S.S. Shinde, T.K. Gundu Rao, B.C. Bhatt, Energy transfer process in $CaSO_4$: Tb, Ce phosphor, J. Lumin. 105 (2003) 1–8.

[40] G.D. Xia, S.M. Zhou, J.J. Zhang, S.M. Wang, J. Xu, Solution combustion synthesis, structure and luminescence of $Y_3Al_5O_{12}$: Tb^{3+} phosphors, J. Alloys Compd. 421 (2006) 294–297.

[41] B.S. Barros, P.S. Melo, R.H.G.A. Kiminami, A.C.F.M. Costa, G.F. de Sá, S. Alves Jr., Photophysical properties of Eu^{3+} and Tb^{3+}-doped $ZnAl_2O_4$ phosphors obtained by combustion reaction, J. Mater. Sci. 41 (2006) 4744–4748.

[42] Z.Y. Hou, L.L. Wang, H.Z. Lian, R.T. Chai, C.M. Zhang, Z.Y. Cheng, J. Lin, Preparation and luminescence properties of Ce^{3+} and/or Tb^{3+} doped $LaPO_4$ nanofibers and microbelts by electrospinning, J. Solid State Chem. 182 (2009) 698–708.

[43] X.M. Liu, R. Pang, Q. Li, J. Lin, Host-sensitized luminescence of Dy^{3+}, Pr^{3+}, Tb^{3+} in polycrystalline $CaIn_2O_4$ for field emission displays, J. Solid State Chem. 180 (2007) 1421–1430.

[44] N.F. Zhu, Y.X. Li, X.F. Yu, Pechinin synthesis and luminescence properties of $Y_3Ga_5O_{12}$(YGG):Tb thin film, Mater. Lett. 62 (2008) 2355–2358.

[45] S.Z. Lin, Y.L. Yuan, H.T. Wang, R.K. Jia, X.F. Yang, S.J. Liu, Controllable synthesis and luminescence property of $CePO_4$: Tb nanorods, J. Mater. Sci.: Mater. Electron. 20 (2009) 899–904.

[46] Y.Y. Zhang, J.L. Liu, Y.X. Zhu, Y. Shang, M. Yu, X. Huang, Hydrothermal synthesis and luminescence properties of core–shell-structured PS@$SrCO_3$: Tb^{3+} spherical particles, J. Mater. Sci. 44 (2009) 3364–3369.

[47] Z.W. Liu, Y.L. Liu, Synthesis and luminescent properties of a new green afterglow phosphor $CaSnO_3$: Tb, Mater. Chem. Phys. 93 (2005) 129–132.

[48] Z.H. Xu, Y.X. Li, Z.F. Liu, D. Wang, UV and X-ray excited luminescence of Tb^{3+}-doped $ZnGa_2O_4$ phosphors, J. Alloys Compd. 391 (2005) 202–205.

[49] L.H. Huang, X.J. Wang, H. Lin, X.R. Liu, Luminescence properties of Ce^{3+} and Tb^{3+} doped rare earth borate glasses, J. Alloys Compd. 316 (2001) 256–259.

[50] D. Wang, Y.H. Wang, Luminescence properties of $LaPO_4$: Tb^{3+}, Me^{3+} (Me = Gd, Bi, Ce) under VUV excitation, Mater. Res. Bull. 42 (2007) 2163–2169.

[51] X.Y. Bai, G.C. Zhang, P.Z. Fu, Photoluminescence properties of a novel phosphor, $Na_3La_9O_3(BO_3)_8$:RE^{3+} (RE = Eu, Tb), J. Solid State Chem. 180 (2007) 1792–1795.

[52] J.Y. Kuang, Y.L. Liu, B.F. Lei, Effect of RE^{3+} as a co-dopant in long-lasting phosphorescence $CdSiO_3$: Mn^{2+} (RE = Y, La, Gd, Lu), J. Lumin. 118 (2006) 33–38.

[53] B.F. Lei, Y.L. Liu, J. Liu, Z.R. Ye, C.S. Shi, Pink light emitting long-lasting phosphorescence in Sm^{3+}-doped $CdSiO_3$, J. Solid State Chem. 177 (2004) 1333–1337.